Science in China Series G: Physics, Mechanics & Astronomy

www.scichina.com
phys.scichina.com
www.springerlink.com

Spin-glass like behaviors in $La_{1-X}Tb_XMnO_3$ perovskite

ZHANG YingTang[1,2,3], WANG ChunChang[2,4], LIU WeiBin[1], WANG Zhong[3], LU HuiBin[2] & CHEN ZiYu[1†]

[1] Department of Physics, Beijing University of Aeronautics and Astronautics, Beijing 100191;
[2] Institute of Physics & Center for Condensed Matter Physics, Chinese Academy of Sciences, Beijing 100190;
[3] School of Material Science & Engineering, Shaanxi University of Technology, Hanzhong 723003;
[4] Institute of Superconducting and Electronic Materials, Wollongong University, Northfield Ave, Gwynneville, NSW 2522, Australia.

A seris of samples of $La_{1-x}Tb_xMnO_3$ ($0 \leqslant x \leqslant 0.15$) are prepared. The static and dynamic magnetizations of $La_{1-x}Tb_xMnO_3$ have been investigated. The results indicate that the spins with the short-range order are frozen into random direction at low enough temperatures which leads to the samples exhibiting the spin-glass like behavior. It is considered that the spin-glass like behavior originates from the competition between ferromagnetic double exchange among Mn^{3+} and Mn^{2+} and antiferromagnetic superexchange among Mn^{3+} and Mn^{3+}, as well as Tb^{3+} and Tb^{3+}.

$La_{1-x}Tb_xMnO_3$, spin-glass-like behavior, short-range order

Perovskite oxides have been investigated due to their peculiar properties[1−3]. Lanthanum manganite ($LaMnO_3$) is the most important category material in the perovskite. When $LaMnO_3$ is doped with divalent cations, it exhibits a range of extraordinary magnetic, electrionic, and structural properties including colossal negative magnetoresistance and charge ordering[4−6], and more. Meantime, doped-$LaMnO_3$ maganites have the complex magnetic phase diagram[7,8]. The phase diagram includes paramagnetic (PM), ferromagnetic (FM), antiferromgnetic (AFM) phase, noncollinear spin ordering (NL-SO) phase, and spin-glass (SG) phases. Recently, there is a resurgence of interest in the manganites because some of them exhibit the particular spin-glass- like (SGL) behavior[9,10]. The concept "spin glass" has been given rise to the work on dilute alloys in the beginning[11−13]. It was applied to describe the phenomenon that by lowering the temperature the impurity spins "freeze out" or become "locked" in random direction in zero external field, i.e., the vector average of all local moments gives no net macroscopic moment, and there is no long – range magnetic order. Nevertheless, there are also the phenomena of SG behavior in some of doped - $LaMnO_3$ maganites. They take on the most prominent features of SG: (1) The "cusp" in the low-field AC and DC magnetizations at the "freezing temperature"; (2) The characteristic of irreversible magnetization at below T_f. Currently, spin-glass like behavior is observed in some perovskite oxides, such as $(La_{1-x}Dy_x)_{0.7}Ca_{0.3}MnO_3$[14], $(Tb\text{-}La)_{2/3}Ca_{1/3}MnO_3$[15], $L_{0.5}Sr_{0.5}CoO_3$ (L = La, Pr, Nd, Sm, and Eu)[16], and $LBaMn_2O_{6-y}$ (L = Pr, Nd, Sm, Eu, Gd, and Tb)[17]. However, the fundamental question whether the maganites with the unusual glassy phenomena can be classified as a classical SG still remains open.

In this letter, the magnetic properties of $La_{1-x}Tb_xMnO_3$ ($0 \leqslant x \leqslant 0.15$) (LTMO) have been investigated. The results indicate that LTMO samples feature unusual SGL behavior, the origin of this feature is also discussed.

Samples of LTMO compounds were prepared by

Recieved March 3, 2009; accepted June 17, 2009
doi: 10.1007/s11433-009-0307-7
†Corresponding author (email: chenzy@buaa.edu.cn)
Supported by the National Natural Science Foundation of China (Grant No. 10334070 and 50871007)

Citation: Zhang Y T, Wang C C, Liu W B, et al. Spin-glass like behaviors in $La_{1-x}Tb_xMnO_3$ perovskite. Sci China Ser G, 2009, 52(12): 1-5, doi: 10.1007/s11433-009-0307-7

conventional solid-state reaction method. Stoichiometric mixtures of high-purity Tb_4O_7, MnO_2 and La_2O_3 powders were ground, palletized, and sintered at 1300℃ in air for 24 h. The crystalline structure of the samples was examined by X-ray diffraction (XRD) measurement with Cu/K radiation ($\lambda = 1.5406$ Å). The AC and DC magnetic measurements were performed in the Superconducting Quantum Interference Device (SQUID) Magnetometer. Measurements of magnetization versus temperature (M-T) were studied between 5 and 300 K following two different protocols: Zero field cooled (ZFC) and field cooled (FC). The ZFC magnetization was obtained by cooling the sample to 5 K in zero field, and turning on a weak magnetic field (H = 50 Oe), then measuring the magnetization as the sample warmed up to 300 K. The FC magnetization was obtained by cooling the sample to 5 K in the magnetic field of 50 Oe, then measuring the magnetization under the same magnetic field as the sample warmed up to 300 K. Magnetization versus field (*M-H*) measurements were performed under the magnetic field between –2 and 2 kOe at different temperatures. The temperature dependence of AC magnetization at different frequencies were studied between 5 and 200 K under the DC magnetic field of 50 Oe and the AC magnetic field of 15 Oe.

Figure 1 shows the XRD patterns of the LTMO (x = 0.05, 0.1 and 0.15) samples. The observed peaks for the samples of $x = 0.05$, 0.1 and 0.15 can be indexed on the basis of the cubic unit cell of space group $Pm\bar{3}m$. In samples of $x = 0.05$, 0.1 and 0.15, it can be seen that the lattice parameters are all slightly decreased with the increasing of doping concentration to 0.15 because the radii of Tb^{3+} is shorter than that of La^{3+}.

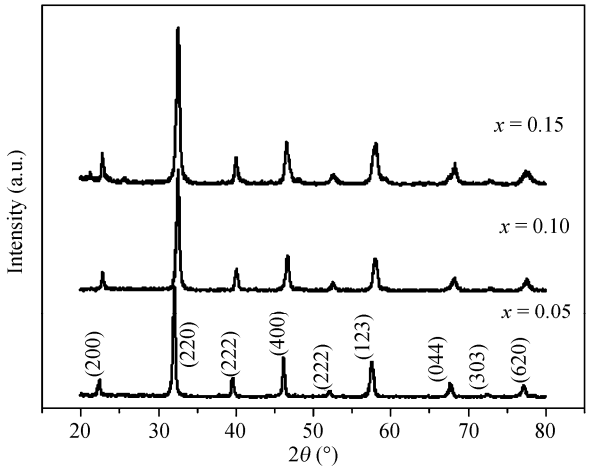

Figure 1 X-ray diffraction patterns of the LTMO ($0 \leqslant x \leqslant 0.15$).

The temperature dependences of DC magnetization under the ZFC and FC conditions for LTMO are shown in Figure 2. The samples show an irreversible thermo-magnetization process below around 150 K, that is, there is an obvious difference between the ZFC and FC curves. The branch temperature (T_{SGL}) increases slightly as the Tb content increases.

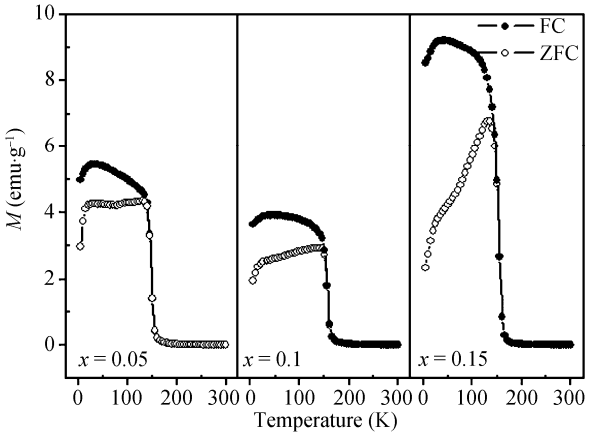

Figure 2 DC ZFC (open symbols) and FC (closed symbols) curves of magnetization of polycrystalline LTMO ($0 \leqslant x \leqslant 0.15$) under an applied field of 50 Oe.

The $M(T)$ curves (FC and ZFC) indicate that the phase transitions from SGL to AFM occur at 20 K. For small substitution concentrations of Tb, the AFM appears under T_N (=20 K). When the temperature is below T_N, the magnetic properties come from superexchange between Tb^{3+} and Tb^{3+} or that of Mn^{3+} ions[18]. Moreover, it can be seen that the systems show a clear trend towards SGL behavior with increasing Tb concentration .

The *M-H* curves for sample of $x = 0.05$ are shown in Figure 3. The *S*- shaped behavior occurs and the irreversibility is observed in *M-H* curves in the temperature range below T_{SGL}. However, there exists a wide variation in the ferromagnets behavior. We see the curves of minor magnetic and open magnetic hystersis loop shown in the lower inset of Figure 3. From the initialization magnetization curves shown in the upper inset of Figure 3, we note that the curves still do not reach saturation values under 0.2 T. This complicated behavior may occur in systems where antiferromagntic and ferromagnetic orderings compete.

Figure 4 shows the temperature dependence of ZFC AC linear magnetization (AC-LM) for sample of x =

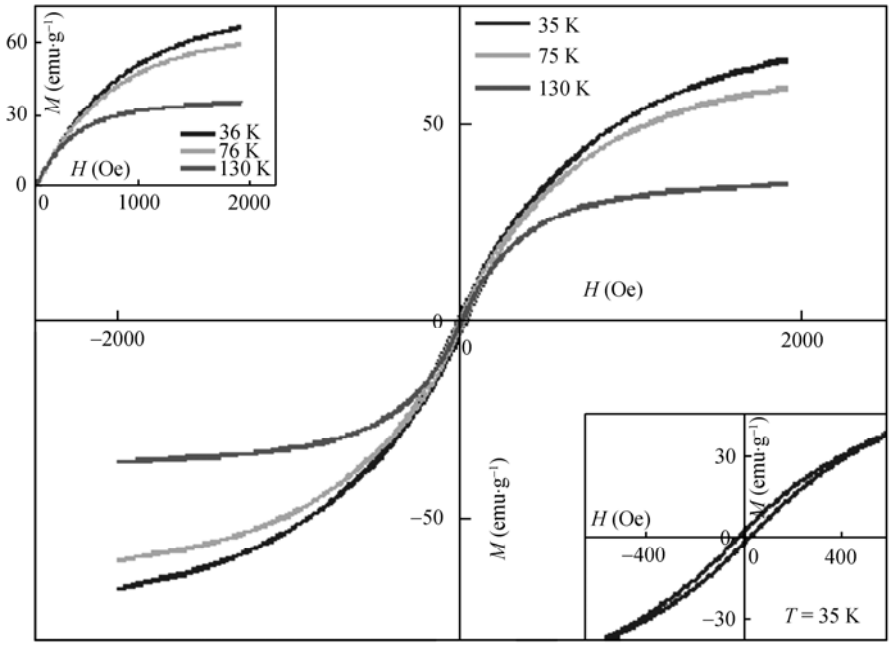

Figure 3 The magnetization curves of LTMO ($x = 0.05$) at various temperatures. The lower inset is the curves of minor magnetic hysteresis loop. The upper inset shows the initialization magnetization curves of LTMO ($x = 0.05$) at several temperature.

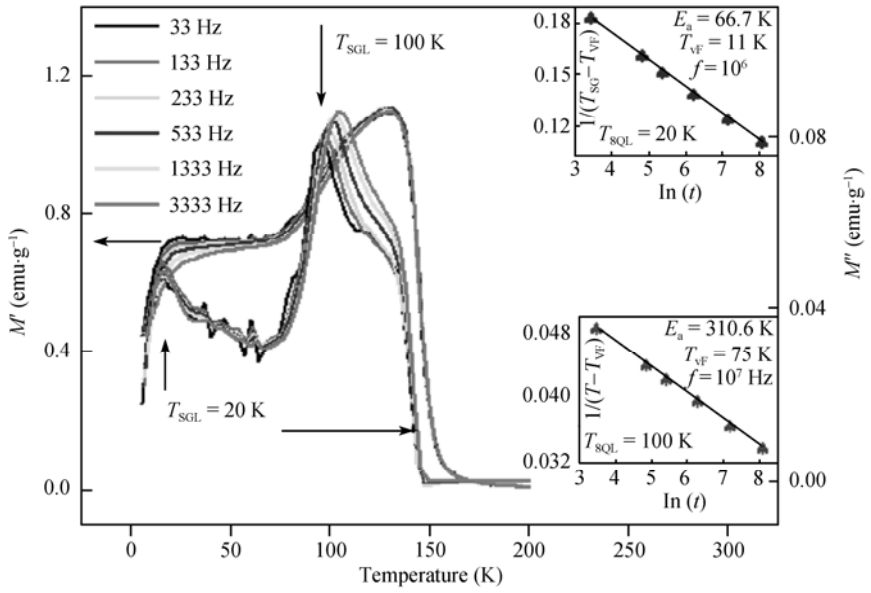

Figure 4 Temperature dependence of the AC-LM of LTMO ($x = 0.05$). M' and M'' are the real and imaginary parts of magnetization, respectively. The upper and lower insets give the fits of T_{SGL} obtained from against frequency using VF law at 100 and 20 K, respectively.

0.05 measured at different frequencies. The sharp peaks at around 20 and 100 K observed in the imaginary curves are consistent with the result of DC magnetization. The AC-LM attains a maximum at T_{SGL}. The T_{SGL} shifts towards higher temperatures with increasing frequencies. This behavior is similar to that of a conventional spin glass. With the temperature decreasing from the PM state, the relaxation time of the SGL state slows down leading to a divergence at T_{SGL}. In order to understand this behaviour, the T_{SGL} as a function of frequency of the two peaks was plotted using the phenomenological Vogel-Fulcher (VF) law[10], $f = f_0\exp(-E_a/k_B(T_{SG} - T_{VF}))$, where E_a and T_{VF} are the activation energy and the VF temperature, respectively. The best fittings displayed

by solid lines in the inset of Figure 4 yield with E_a = 66.7 K and T_{VF} = 11 K for peak around 20 K and E_a = 310.6 K, T_{VF} = 75 K for peak around 100 K, respectively. The values of the characteristic frequencies, f_0, are found to be ~10^6 Hz and 10^7 Hz for the peaks at around 20 and 100 K, respectively, which are smaller than the value of ~10^{13} Hz, typically taken for SG compounds[19].

In order to identify whether or not a true thermodynamic spin glass phase transition occurs in LTMO, we have investigated the ZFC AC nonlinear magnetization (AC-NLM, M'_{nl}). The results about the AC-NLM for sample of $x = 0.05$ as functions of temperature and frequency are shown in Figure 5. As the AC-NLM is in relation with the spin-glass order parameter, the critical behavior of the AC-NLM is regarded as a crucial evidence for the spin-glass phase transition. The AC-NLM is expected to show a power-law in the form of $M_{nl} \propto \left((T - T_{SGL})/T_{SGL}\right)^{-\gamma}$ $(\gamma > 0)$[21] as temperature is close to T_{SGL}. Based on this piont, $M_{nl}(T)$ related with the temperature and frequency might be described as $M_{nl} = \alpha((T - T_{SGL})/T_{SGL})^{-\gamma} - \beta(\omega)$, where α and $\beta(\omega)$ are constants, γ is a critical exponent which represents a phase transition. The value of critical exponent γ is equal to the estimated $1 \leqslant \gamma \leqslant 2$[20] or $3 \leqslant \gamma \leqslant 4$[21] for a SG system. It is seen from the inset of Figure 5 that the simulation is consistent with the experimental data based on a power-law. From the simulations, the values of critical exponent γ of LTMO ($x = 0.05$) at different frequencies are deduced to $1.8 \leqslant \gamma \leqslant 1.9$, the values of α are found to be 3×10^{-4}, and the values of $\beta(\omega)$ are found to be 5.1×10^{-3}, 4.93×10^{-3}, 4.53×10^{-3}, 4.4×10^{-3}, 3.2×10^{-3} and 0 at frequencies of 33, 133, 233, 533, 1333, and 3333 Hz, respectively. There is the feature of magnetic relaxation. These results indicate that a thermodynamic glass phase transition occurs in LTMO.

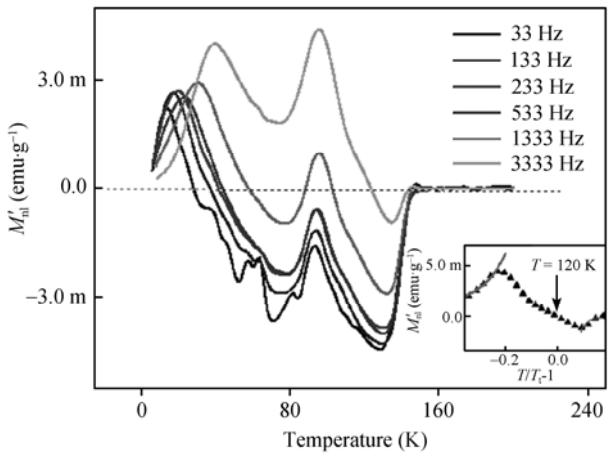

Figure 5 The AC-NLM of LTMO ($x = 0.05$) as a function of temperature measured at several frequencies in the temperature range from 5 K to 200 K. The amplitude of the AC field is 15 Oe. The simulations are shown as solid lines in the inset.

Based on the above results, the T-x phase diagram for LTMO is presented in Figure 6. During 20–150 K range, the SGL behaviors can be ascribed to the competition between FM double exchange (DE)[22] between Mn^{3+} and Mn^{2+} and AFM superexchange between Mn^{3+} and Mn^{3+} and in addition, Tb^{3+} and Tb^{3+}. In addition, since Tb ions may not involve in DE processes with Mn ions, higher Tb substitutions should lead to the formation Tb-O-Tb coupling, which leads to stronger suppression of the ferromagnetism. Therefore, the system shows a clear trend towards SGL behavior with increasing Tb concentration.

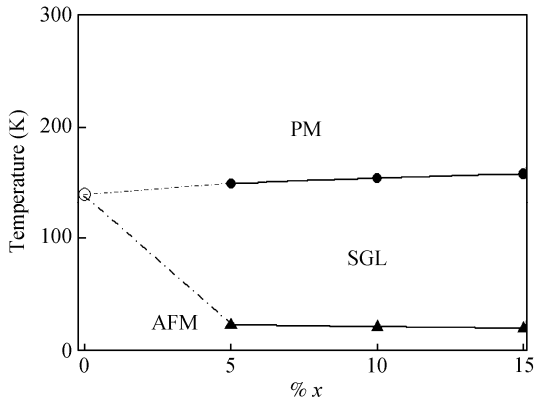

Figure 6 *T-x* phase diagram of LTMO: PM, paramagnetic phase; AFM, antiferromagnetic phase; SGL, spin glass like phase. "○" denotes the data from ref. [23].

In summary, we have studied the structural and magnetic properties of $La_{1-x}Tb_xMnO_3$ ($0 \leqslant x \leqslant 0.15$) system. The results indicate that the system exhibits the spin-glass-like feature. This feature is believed to be related to the competition between ferromagnetic double exchange among Mn^{3+} and Mn^{2+} and antiferromagnetic superexchange among Mn^{3+} and Mn^{3+} as well as Tb^{3+} and Tb^{3+}.

1 Moreno L C, Valencia J S, Tellez D A L. Preparation and structural study of $LaMnO_3$ magnetic material. J Magn Magn Mater, 2008, 320: e19—e21

2 Royer S, Levasseur B, Alamdari H. Mechanism of stearic acid oxi-

dation over nanocrystalline $La_{1-x}A_xBO_3$ (A = Sr, Ce; B=Co, Mn): The role of oxygen mobility. Appl Catal B-Environ, 2008, 80: 51－61
3 Koubaa W C R, Koubaa M, Cheikhrouhou A. Structural, magneto-transport, and magnetocaloric properties of $La_{0.7}Sr_{0.3-x}Ag_xMnO_3$ perovskite manganites. J Alloy Compd, 2008, 453: 42－48
4 Gorbenko O Y, Kaul A R, Babushkina N A. Giant magnetoresistive thin films of $(La,Pr)_{0.7}(Ca,Sr)_{0.3}MnO_3$ prepared by aerosol MOCVD. J Mater Chem, 1997, 7: 747－752
5 Millis A J. Cooperative Jahn-Teller effect and electron-phonon coupling in $La_{(1-x)}A_{(x)}MnO_{(3)}$. Phys Rev B, 1996, 53: 8434－8441
6 Satpathy S, Popovic Z S, Vukajlovic F R. Electronic structure of the perovskite oxides: $La_{1-x}Ca_xMnO_3$. Phys Rev Lett, 1996, 76: 960－963
7 Jia Y X, Lu L, Khazeni K, et al. Magnetotransport properties of $La_{0.6}Pb_{0.4}MnO_{3-\delta}$ and $Nd_{0.6}(Sr_{0.7}Pb_{0.3})_{0.4}MnO_{3-\delta}$ single crystals. Phys Rev B, 1995, 52: 9147－9150
8 Yamada Y, Hino O, Nohdo S, et al. Polaron ordering in low-doping $La_{1-x}Sr_xMnO_3$. Phys Rev Lett, 1996, 77: 904－907
9 Nakamura S, Soeya S, Ikeda N, et al. Spin-glass behavior in amorphous $BiFeO_3$. J Appl Phys, 1993, 74: 5652－5657
10 De K, Patra M, Majumder S, et al. Spin-glass like features in cluster-glass compounds $La_{1-\delta}Mn_{0.7}Fe_{0.3}O_3$. J phys D-Appl Phys, 2007, 40 (24): 7614－7619
11 Mizoguchi T, McGuire T R, Kirkpatrick S, et al. Measurement of spin-glass order parameter in amorphous $Gd_{0.37}Al_{0.63}$. Phys Rev Lett, 1977, 38(2): 89－92
12 Takahashi M, Sembiring T, Noda Y, et al. Magnetic structures and pin-glass-like behavior in ordered and disordered Pt-rich Pt-Mn alloys. Phys Rev B, 2004, 70: 014431
13 Baker P J, Battle P D, Blundell S J, et al. Synthesis and characterization of two metallic spin-glass phases of $FeMo_4Ge_3$. Phys Rev B, 2008, 77: 134405
14 Yusuf S M, Chakraborty K R, Paranjpe S K, et.al. Magnetic and electrical properties of $(La_{1-x}Dy_x)_{0.7}Ca_{0.3}MnO_3$ perovskites. Phys Rev B, 2003, 68: 104421
15 de Teresa J M, Ibarra M R, Garcıa J, et al. Spin-Glass Insulator State in $(Tb\text{-}La)_{2/3}Ca_{1/3}MnO_3$ perovskite. Phys Rev Lett, 1996, 76: 3392－3395
16 Yoshii K, Abe H. Doping effects of Ru in $L_{0.5}Sr_{0.5}CoO_3$ (L=La, Pr, Nd, Sm, and Eu). Phys Rev B, 2003, 67: 094408
17 Trukhanov S V, Troyanchuk I O, Hervieu M, et al. Magnetic and electrical properties of $LBaMn_2O_{6-\delta}$ (L=Pr, Nd, Sm, Eu, Gd, Tb) manganites. Phys Rev B, 2002, 66: 184424
18 Xiang H J, Wei S H, Whangbo M H, et al. Spin-orbit coupling and ion displacements in multiferroic $TbMnO_3$. Phys Rev Lett, 2008, 101(3): 037209
19 Binder K, Young A P. Spin glasses: Experimental facts, theoretical concepts, and open questions. Rev Mod Phys, 1986, 58: 801－976
20 Barbara B, Malozemoff A P, Imry Y. Scaling of nonlinear susceptibility in MnCu and GdAl spin-glasses. Phys Rev Lett, 1981, 47: 1852－1855
21 Monod P, Bouchiat H. Equilibrium magnetization of a spin-glass is mean-field theory valid. J Phys Lett, 1982, 43(2): 45－53
22 Yang J, Ma Y Q, Zhang R L, et al. Structural, transport, and magnetic properties in the Ti-doped manganites $LaMn_{1-x}Ti_xO_3$ ($0<x<0.2$). Solid State Commun, 2005, 136: 268－272
23 Coey J M D, Viret M, Molnar S V. Mixed- valence manganites. Adv Phys, 1999, 48: 167－293